16th World Conference on Earthquake, 16WCEE 2017

Santiago Chile, January 9th to 13th 2017

Paper N° 3890

Registration Code: S-K1464659251

INVESTIGATING THE EFFECT OF SOIL-STRUCTURE INTERACTION ON COLLAPSE OF INTEGRAL ABUTMENT BRIDGES

K. Ashkani Zadeh [(1)], C. E. Ventura [(2)]

[(1)] *PhD Student, The University of British Columbia, Vancouver, Canada, kianosh@civil.ubc.ca*

[(2)] *Professor, The University of British Columbia, Vancouver, Canada, ventura@civil.ubc.ca*

Abstract

In this study, a performance based approach is employed to investigate the effect of soil-structure interaction (SSI) on the response of integral abutment bridges. Non-linear Incremental Dynamic Analysis (IDA) is used for the analysis the structure and to generate fragility curves for this type of bridge. Finite element models are constructed for three types of integral abutment bridges. Simulation are performed considering and neglecting the SSI effects. A total of 20 selected ground motions was used in the IDA of the bridge models. The spectral acceleration of ground motions is chosen as the Intensity Measure (IM) and relative displacement and drift of the abutment back walls and pier columns are chosen as engineering demand parameters (EDPs). The Collapse Margin Ratio (CMR) is chosen as a measure to objectively compare the response of non-SSI and SSI models. In the cases studied here, the SSI models showed significant reduction in collapse margin ratio when compared to their counterpart non-SSI model. This indicates that ignoring the soil effect may result in under estimation of the probability of collapse.

Keywords: Integral Abutment Bridges; Soil Structure Interaction (SSI); Incremental Dynamic Analysis (IDA); Collapse Margin Ratio (CMR); Probability of Collapse.

1. Introduction

Several bridges have collapsed worldwide as a result of strong earthquakes (e.g. [1]). lack of understanding of soil-structure interaction (SSI) is one of several reasons for such collapses. As discussed by [1] and [2], soil-pile-structure interaction has led to damage and rupture of bridge piers in Northridge Earthquake in 1994. Collapse of the 630-meter long Hanshin Expressway Bridge during the Kobe Earthquake in 1995 is another example of the contribution of SSI [18]. An analytical study of the Hanshin Expressway showed that soil characteristics had a significant effect on the behaviour of this structure [3]. The inertial SSI effect also had led to elongation of bridge's fundamental periods resulting in a more severe response. Similar phenomenon was observed in the collapse of the Cypress Bridge in Oakland during the Loma Prieta earthquake in 1989 [4].

Current seismic design codes are lacking comprehensive provisions to deal with the SSI effects [4]. In the National Building Code of Canada (NBCC2015) [5], the effect of soft soil on the response spectrum is incorporated via the F_α and F_v site response coefficients.

However, the contribution of SSI effects on the structural response needs to be effectively addressed in the next generation of bridge design codes to minimize seismic risk and avoid catastrophic failure of bridges.

In this study, the Incremental Dynamic Analysis (IDA) method is used as part of a methodology developed to investigate the effects of soil-structure interaction on the potential collapse of integral abutment bridges, within a performance-based framework. The Collapse Marginal Ratios (*CMR*) introduced by FEMA P-695 [6] as a collapse measure for buildings is adopted here to bridge structures. CMR is used to compare the performance of SSI and non-SSI models. Further information on the methodology and approach used for the study conducted by the authors can be found in [7].

2. Methodology

The proposed methodology consists of three steps:

- Step1: Model construction and analysis,
- Step 2: Calculation of probability of collapse,
- Step 3: Interpretation and comparison of collapse margin ratios.

An incremental dynamic analysis is performed using a set of selected ground motions on detailed FE models of the bridges. Probability of collapse is then calculated from the IDA analysis outputs and used to construct the fragility curves. The collapse margin ratios (*CMR*) are then predicted for each set of analysis. A schematic of the methodology adopted here is presented in Fig.1.

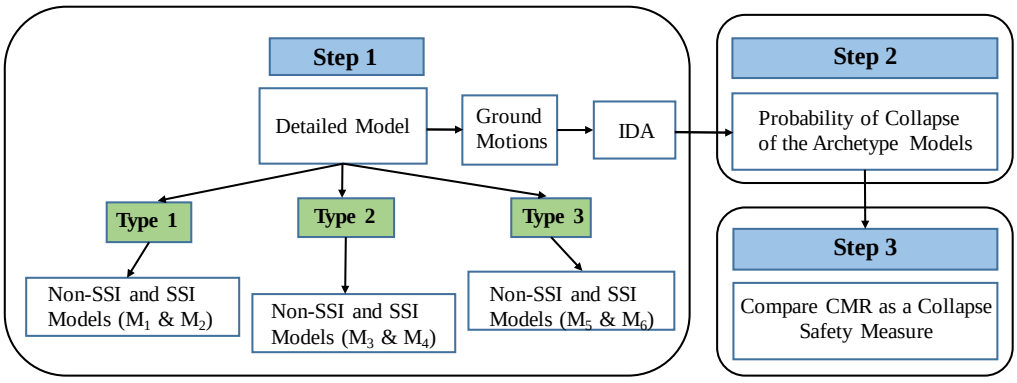

Fig. 1 – General framework of the study research

2.1 Model Construction and Analysis (Step 1)

In this step, a detailed finite element model of each of the bridge archetypes is developed. A set of suitable ground motions is selected and the IDA analysis is performed on the models. Details of model construction and analysis is described below.

2.1a FE Model construction

The SeismoStruct software is employed to develop the 3-D nonlinear models of integral abutment [8]. Geometric non-linearity, as well as, non-linear behaviour of primary structural elements is considered in the model.

Two archetype models are developed for each bridge: one considering the SSI effects and another one without considering it. In the SSI models, the effect of soil-structure interaction from soils supporting the piles and abutment backwalls are taken into account. The SSI p-y link introduced by is employed here to simulate the effect of soil surrounding piles. The properties of soil sub-layer models are considered in determining the link properties. The effect of the soil behind the abutment backwall is simulated using springs as recommend by the CALTRANS guidelines [9].

The p-y links include features such as loading and unloading rules, modeling of radiation damping and cyclic degradation, and slack zone for the analysis of shallow and deep foundation [10]. The properties of p-y link are determined based on properties of soil according to API code recommendations for load-deflection (p-y) curves for Sand and soft clay [11] and L-Pile reference manual [12] for stiff clay layer based on Reese model for stiff clay without water.

Ga2.1b Ground motions

FEMA P-695 [6] recommendations are employed to select a set of 20 selected ground motions from the PEER Strong Motion database.

According to FEMA P-695, ground motions whose response spectrum best fits to mean site spectrum are chosen. The selected ground motions were applied to the models without any modification or scaling at the period of vibration of the bridges in the analysis. To produce the fragility curves using Incremental Dynamic Analysis (IDA), intensity of ground motions is increased until structural failure occurs. Period of interest is considered the range between smallest and biggest period of the bridge models. Response spectra for five out of the twenty selected ground motions and the target spectrum along with the period of interest are shown in Fig. 2. Vancouver's Uniform Hazard Spectrum (UHS) is also shown in the figure for comparison. To estimate UHS, Vs30 is considered based on NBCC 2005 soil site class C, with an average shear wave velocity of 360-750 m/s.

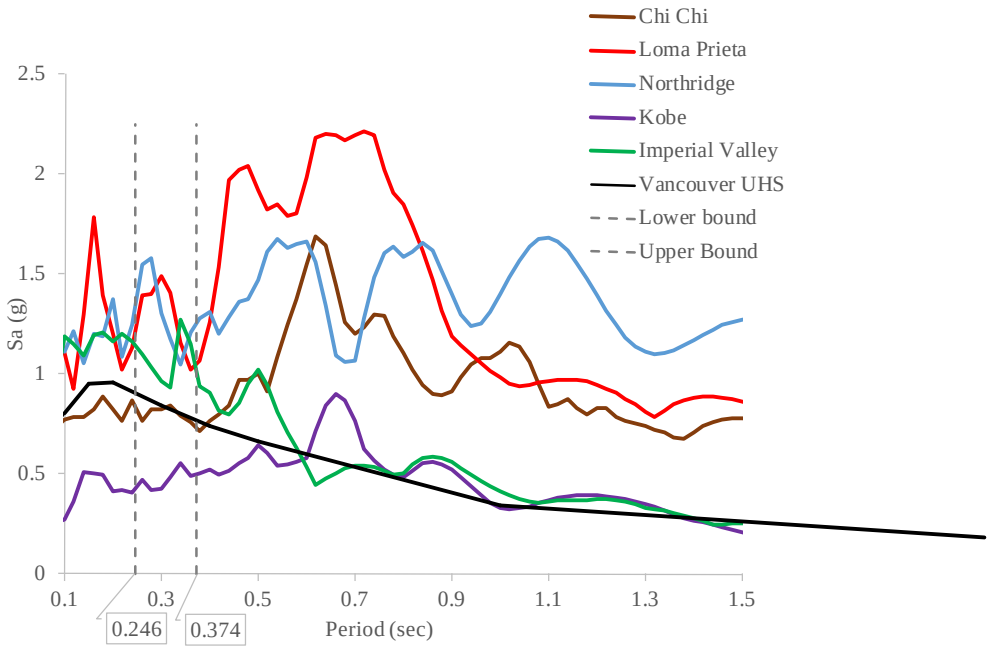

Fig. 2 – Ground motion spectra along with the target spectrum (2% in 50 years and 5% damping), and the range of period of interest

2.1c Incremental Dynamic Analysis (IDA)

In the Incremental Dynamic Analysis method (IDA), the structure is subjected to a sequence of excitations of increasing intensity. The analysis is continued until the structure reaches a pre-defined collapse state. The median collapse intensity can be extracted from IDA analysis [14]. Collapse conditions and the collapse fragility curves are then calculated for each archetype model using a cumulative distribution function (CDF).

In this study, a coefficient of 0.25 was used as the initial multiplier and further increments are performed using a 0.25 increase at each stage. Acceleration time histories are applied in directions transverse and perpendicular to the bridge decks.

Spectral acceleration is chosen as the intensity measure (IM) here and drifts of the abutment backwalls and pier columns are considered as engineering demand parameters (EDPs). The main objective here is the evaluation of performance of the seismic-force resisting system. To achieve this purpose, performance criteria are evaluated based on 'collapse prevention' according to FEMA P-695.

In this study, the event of collapse is not simulated explicitly; instead, non-simulated collapse modes are evaluated using limit state checks on structural response quantities calculated in the analyses (performance criteria).

In non-simulated collapse modes, failure of the first primary structural component is assumed as an indicator of structural collapse. As discussed in FEMA P-695, non-simulated limit state checks may result in lower estimates of the median collapse compared to the case that all the local failure modes are directly simulated [6].

2.2. Probability of Collapse (Step 2)

Fragility curves are calculated based on the results of the IDA analyses. Probability of collapse is calculated as a function of spectral acceleration (S_a). As suggested by [15], a log-normal cumulative distribution function is fitted to data using least square method.

This approach can be used to fit fragility functions for a variety of situations, particularly, collapse fragility functions obtained from structural analysis data. A CDF is fitted to IDA data, to provide a continuous estimate of the probability of collapse as a function of S_a using the following equation:

$$P(C \mid S_a = x) = \Phi\left(\frac{\ln(x/\mu)}{\sigma}\right) \quad (1)$$

where,

$P(C \mid S_a = x)$ is the probability that a ground motion with $S_a = x$ will cause the structure

to collapse,

Φ () is the standard normal cumulative distribution function (CDF),

μ is the median of the fragility function

and σ is the standard deviation of ln S_a or dispersion of S_a

2.3. Collapse Marginal Ratio (*CMR*) (Step 3)

Collapse Margin Ratio (CMR) is defined as the ratio between the median collapse intensity (S_{CT}) and the Maximum Considered Event (MCE) intensity (S_{MT}). MCE intensity (S_{MT}) is obtained from the response spectrum of MCE ground motions at the fundamental period, T_1 [6]. *CMR* is calculated as per Eq. 2 below.

$$CMR = S_{CT} / S_{MT}(T_1) \quad (2)$$

The *CMR* parameter offers an objective indicator for structure collapse. This parameter combines the fragility curve with the site-specific response spectrum. Higher *CMR* values indicate less chance of failure while cases with lower *CMR* values have a higher probability of failure.

3. Bridge Models

In this section a brief discussion of the bridge models selected for this study is provided. Details of how the SSI effects have been incorporated into these models are also presented.

3.1. Archetype Models

Three different types of bridges are considered to calculate and compare the probability of collapse of the integral abutment bridges (see Table 1 for details). Two archetype models namely, SSI and non-SSI models, are defined for each bridge type.

M_1 model corresponds to a simplified model of a single span integral abutment bridge with a 30° skew angle. Fixed support was applied to the base of the foundations of M_1 and all the other non-SSI models. M_2 model is the SSI version of the M_1 model considering effect of soil around the abutment piles assuming a soil sub-layer arrangement along the abutment piles. SSI effects behind the abutment backwall and around the piles are simulated by employing CALTRANS springs [9] and SSI p-y links corresponding to each layer of soil as discussed in section 2.1. In the SSI models, seismic loading was applied to the base of piles. In the non-SSI models, seismic loading was applied to the base of abutment and pier foundations.

M_3 and M_4 models correspond to non-SSI and SSI models of a three-span integral abutment bridge with a 15° skew angle. Finally, M5 and M6 models are the non-SSI and SSI models of a three-span two-band common semi-integral abutment bridge with a 6° skew angle. Fig. 3 shows the schematics of three type bridges studied here.

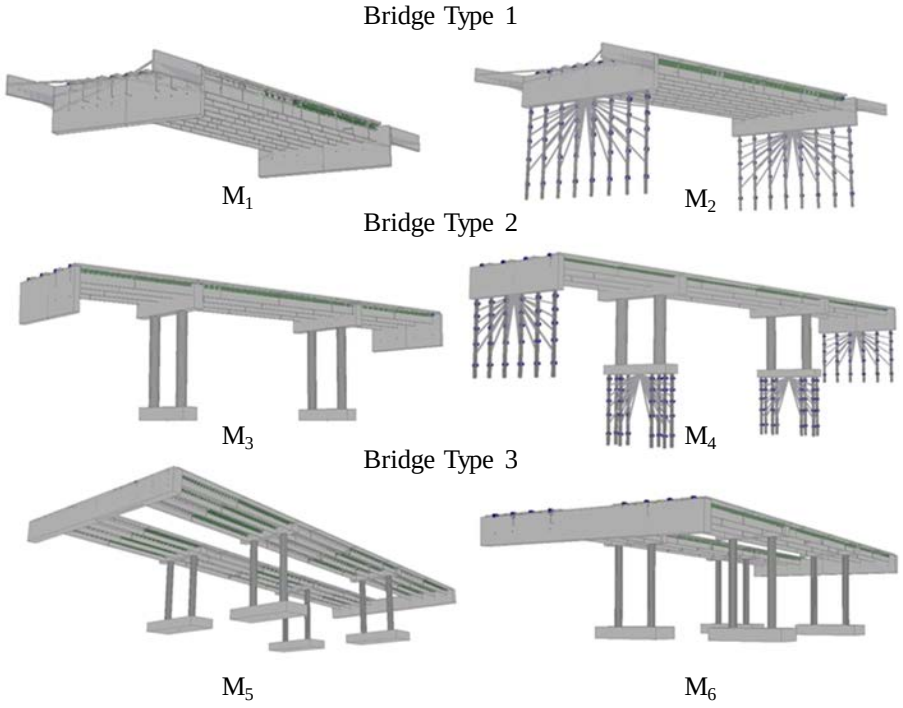

Fig. 3 – Shows different three type of bridges used in this study

Table 1 – Summary of the bridge types and archetype models are developed and used in this study

Archetype Model	Structural Feature	Span Length (m)	Skewness Angle (°)	Horizontal Radius (m)	SSI Feature
M_2	Integral abutment bridge with abutment pile foundations and total 9 pre-stressed precast girders	38	30°	–	CALTRANS springs and SSI p-y links
M_4	Integral abutment bridge with pier & abutment pile foundations and total 4 pre-stressed precast girders	17-29-19	15°	1009.95	CALTRANS springs and SSI p-y links
M_6	Two-band semi-Integral abutment bridge with common seat abutment, pier pilecap deep foundation, intermediate diaphragm, and total 8 pre-stressed precast girders	27.5-37.5-27.5	6°	–	CALTRANS springs

The soil sub-layer arrangement shown in Fig. 4 is considered to account for soil effect around the abutment and pier piles.

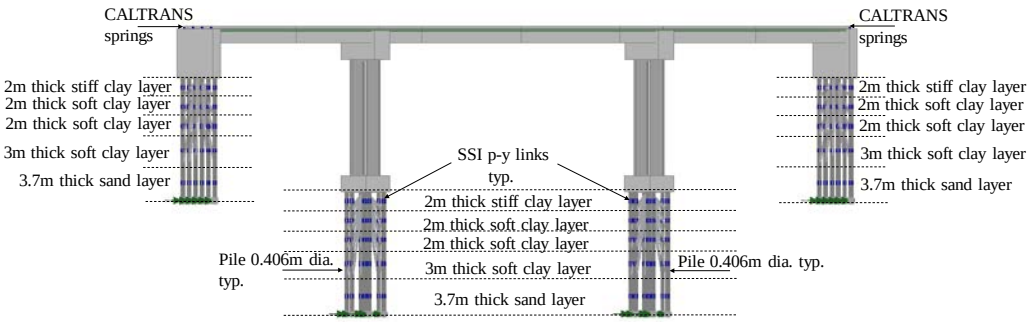

Fig. 4 – Shows assumed soil sub-layer around the piles and location of the assigned CALTRANS springs and SSI p-y links in the SSI models

3.2. SSI model parameters

The sub-layer arrangement as shown in Fig. 5 is based on a geotechnical recommendation report provided by the Hatch Mott MacDonald and MMM Group (H5M joint venture) for the design stage of one of the newly constructed bridges as a part of the Port Mann Highway 1 Project in Vancouver [16].

The API code and L-Pile software manual are employed to develop the p-y curves for clay layers and sand layer, respectively (shown in Fig. 5). The parameters used in SeismoStruct are extracted from the p-y curves. Parameters of the tri-linear backbone p-y curves for each layer are presented in Table 2.

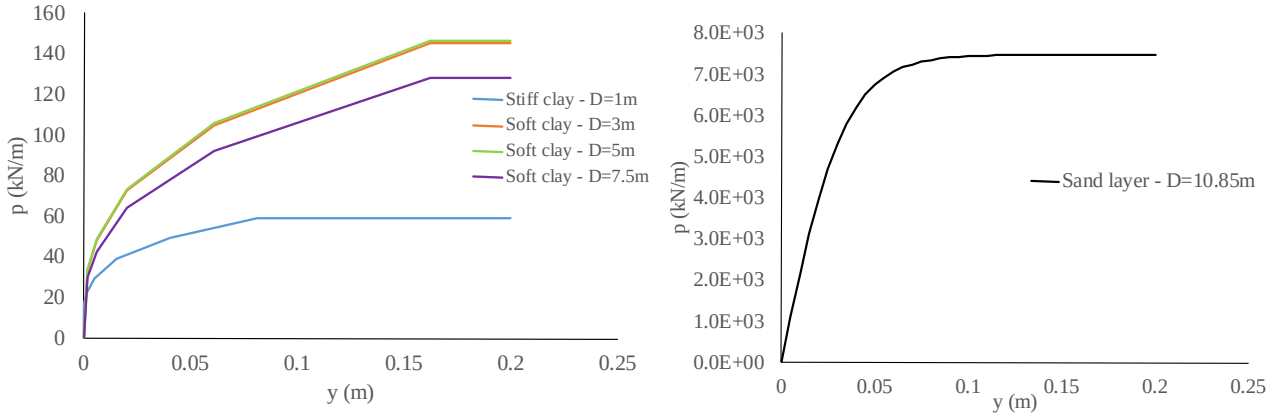

Fig. 5 – (a) Developed p-y curves based on the assumed sub-layers of soil surrounding piles using API code and L-Pile Manual. (b) Obtained p-y curve for sand layer around the piles using API code.

For simplicity, soil layers around the abutment and pier piles are considered to be identical in M_2 and M_4 models.

Table 2 – Calculated parameters which obtained fitting a tri-linear curve to the derived p-y curves

Layer	Thickness (m)	Depth (m)	k_0 (kN/m)	α	B	P_u (kN)	F_y (kN)	$\beta_n=P_u/F_y$	F_c/F_y
Stiff Clay	2	1	11490.6	0.0969	0.040	117.2	98.6	1.189	0.595
Soft Clay	2	3	15651.5	0.1313	0.051	289.3	208.3	1.389	0.458
Soft Clay	2	5	15814.1	0.1313	0.051	292.3	210.5	1.389	0.458
Soft Clay	3	7.5	20756.1	0.1313	0.051	383.7	276.2	1.389	0.458
Silty Sand	3.7	10.85	685185.2	0.3484	0.060	27624.2	25900	1.067	0.714

in which,

k_0 : initial stiffness

α: second segment coefficient of stiffness of the nonlinear dynamic soil structure interaction model

β: stiffness ratio parameter in the SSI model which defines the stiffness of the third segment in proportion to k_0

P_u: soil ultimate strength

F_c: soil strength ratio at first turning point

F_y: soil yield strength

β_n: strength ratio parameter in the SSI model

In this study, to account for the effect of embankment soil behind the abutment backwalls, CALTRANS springs are used in the M_2, M_4 and M_6 models. Stiffness of the abutment due to passive pressure of backfilling behind it is obtained based on section 7.8.1-2 SDC 2013 [9] as per Eq. 3 and summarized in Table 3.

$$k_{abut} = k_i w\left(\frac{h}{1.7\text{m}}\right) \tag{3}$$

where, k_i is the initial stiffness of the embankment fill material behind the abutments, and based on section 7.81-1 of SDC 2013 can be calculated using Eq. 4:

$$k_i \approx \frac{28.7\ \text{kN/mm}}{\text{m}} \quad (4)$$

in which,

w is the projected width of the backwall or diaphragm for seat and diaphragm abutments respectively

h is the effective height of abutment which is determined based on the diaphragm design.

Here, the effective height is chosen assuming that abutment diaphragms are designed for full soil pressure.

Table 3 – Summary of calculated stiffness of the bridge abutments due to the embankment passive pressure force resisting movement

Models	k_i (kN/mm/m)	w (m)	k (m)	$k_{abut.}$ (kN/mm)
M2	28.7	19.2	4.33	1404
M4	28.7	13.69	5.1	1178.54
M6	28.7	34.88	4	2355.43

4. Results

4.1. IDA Results

The maximum pier column relative displacements (displacement between top of pier footing and top of the pier columns) were extracted from IDA simulations at the collapse stage. Fig 6. Shows these relative displacements for M_4 model. Hysteresis loops corresponding to moment vs curvature and base shear vs drift behaviors are also calculated for pier column members. Figure 7 shows the pier column total drift ratio of the M_3 and M_4 models versus total base shear and moment for the Chi Chi ground motion. These graphs correspond to IDA simulations that have resulted in collapse. The M3 curve shows a collapse at a time-history scale factor of 2.0 and the M_4 model shows collapse at scale factor of 0.75.

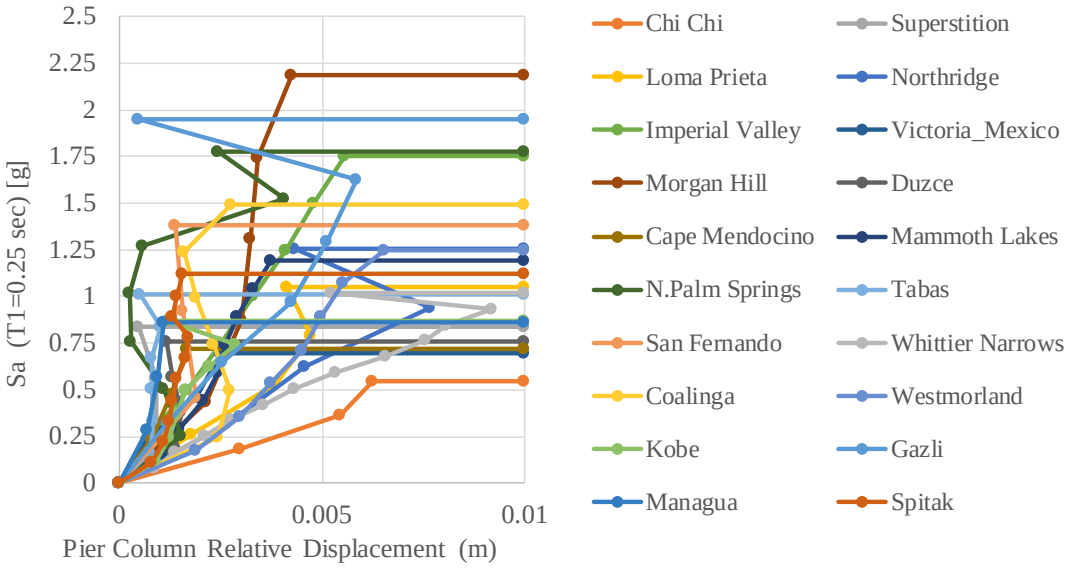

Fig. 6. Predicted pier column relative displacement along the bridge deck for M_4 model.

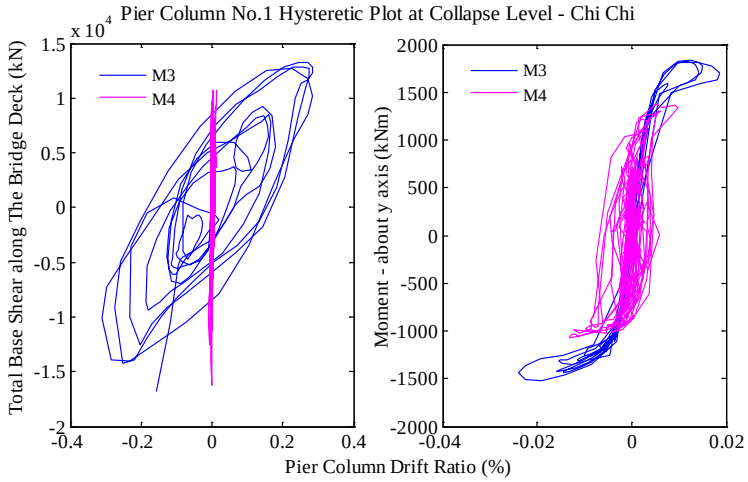

Fig. 7 – Pier column drift ratio across the bridge deck versus (a) total base shear, and (b) total moment calculated using IDA - M_3 and M_4 models.

As shown in Fig. 7, the column's drift for the SSI model (M_4 model) is significantly reduced at the collapse level. Despite of this reduction in column drift, as will be discussed later, probability of collapse is increased in the SSI model for a given earthquake. This is due to the change in failure mode in the SSI models. Fig. 8 shows a summary of the failure modes observed in various bridges based on the IDA simulations. As an example, in the M1 model, failure is mainly due to abutment shear force whereas in its SSI counterpart (M2 Model), the majority of failures are due to girder shear force.

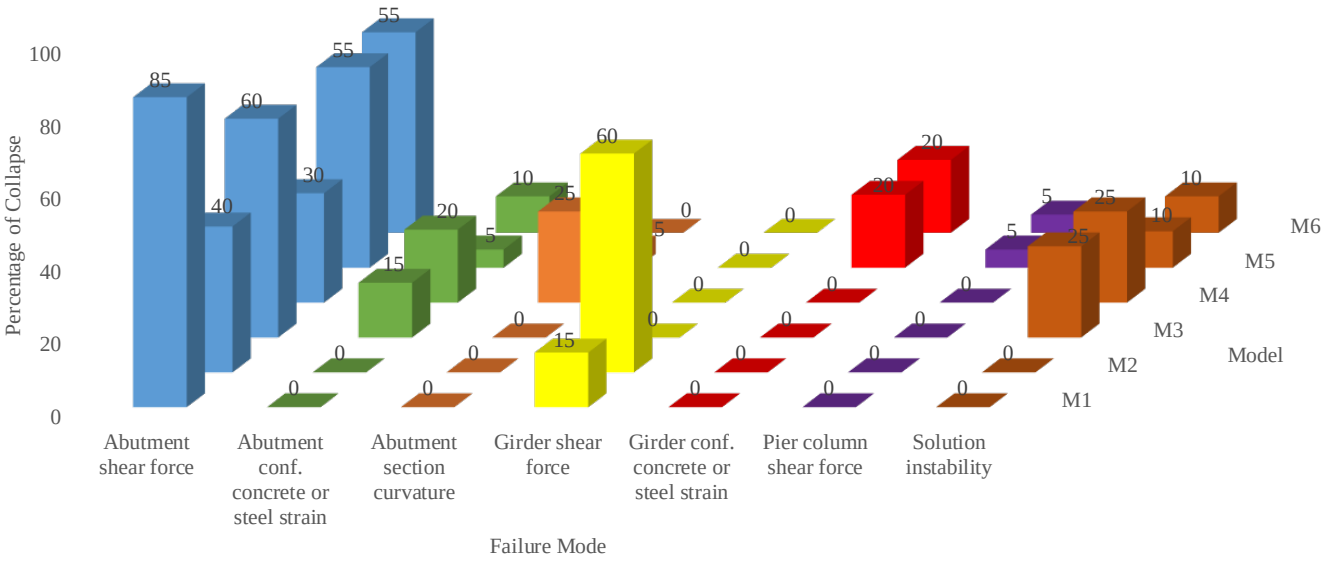

Fig. 8 Percentage share of each failure mode defined as performance criteria in all the model

4.2. Probability of Collapse and Collapse Marginal Ratio (*CMR*) Results

The MATLAB code developed by Baker [17] was employed to calculate the fragility curves. Calculated probabilities of collapse of the archetype models are presented in Fig. 9. Assuming that the shear wave velocity of the top 30m of the site sub-layer soil is between 360m/s and 750m/s, which is equivalent to soil site class C based on [5], collapse margin ratios for 10%, 20%, and 50% (median) were calculated and presented in Table 4.

Although pier drifts predicted in the SSI models (as shown in Fig. 7) are typically smaller than the corresponding non-SSI models, redistribution of load to other components, such as the abutment, has led to

earlier structural failure. This has consequently resulted in shifting the *CMR* curve corresponding to SSI models to the left when compared with the non-SSI counterparts.

As shown in Fig. 9, the SSI model exhibits a reduction in predicted *CMR* values. As a result, for a given S_a, probability of collapse is increased. For instance, the M3 model subjected to the Chi Chi earthquake fails at a S_a, level of 1.61g due to shear force in the abutments, whereas the SSI model of the same bridge (M4 model) has failed at S_a, of 0.54g due to Abutment concrete confinement strain and steel strain. As shown in Fig 10, reduction of CMR in the SSI model has led to an increase in probability of collapse for a given S_a.

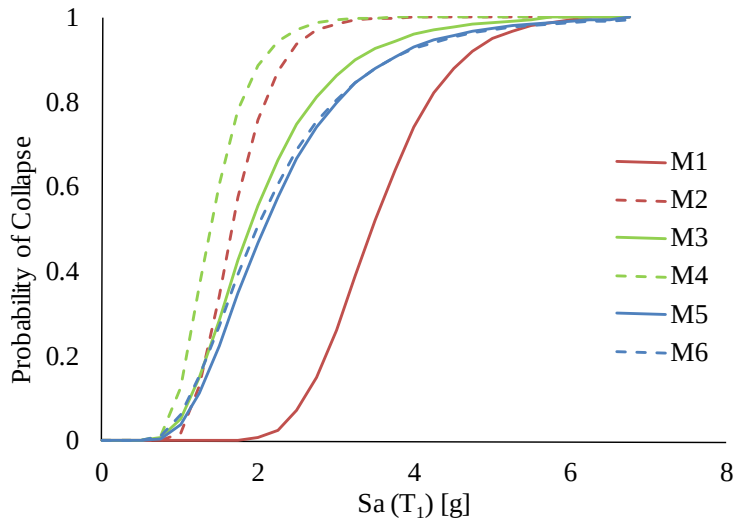

Fig. 9 – Calculated probability of collapse for all the archetype models

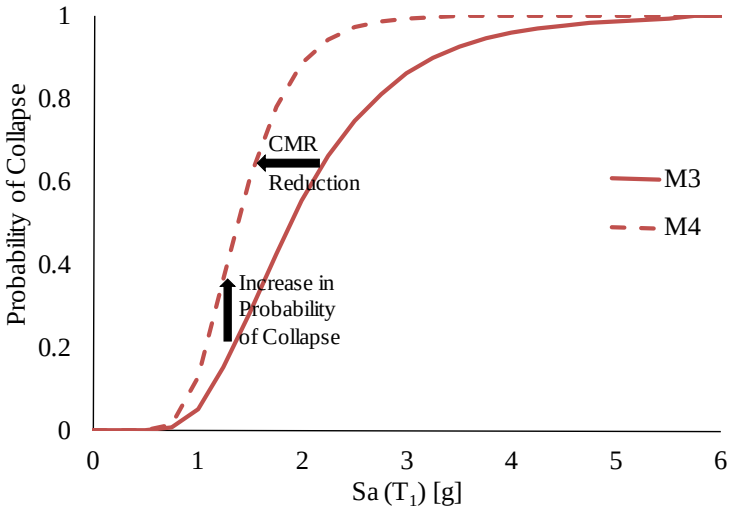

Fig. 10 – Reduction of *CMR* and increase of Probability of Collapse in SSI model

Table 4 – Summary of the calculated collapse margin ratios for median (50%), 10%, and 20% and for all models

Model	T_1 (sec)	$S_{ct\ 10\%}$ (g)	$S_{ct\ 20\%}$ (g)	$S_{ct\ @\ Median}$ (g)	$S_{MT\ @\ T1}$ (g)	$CMR_{10\%}$	$CMR_{20\%}$	CMR_{Median}
M_1	0.25	2.59	2.86	3.46	0.90	2.88	3.18	3.84
M_2	0.28	1.19	1.33	1.67	0.86	1.39	1.56	1.95
M_3	0.34	1.13	1.34	1.90	0.80	1.41	1.68	2.38
M_4	0.37	0.94	1.08	1.39	0.76	1.24	1.42	1.84
M_5	0.37	1.21	1.45	2.08	0.76	1.60	1.91	2.74
M_6	0.37	1.11	1.35	1.99	0.76	1.46	1.78	2.62

5. Conclusions

In this study, Incremental Dynamic Analysis (IDA) within the framework of Performance-based Design was adopted to simulate the response of three bridge models. In all cases, the analyses were carried out with and without considering the SSI effects. A set of 20 selected ground motions were chosen for the IDA analysis.

FEMA P695's non-simulated collapse mode concept was adopted as a collapse indicator. Fragility curves were extracted based on predictions of IDA simulations for both non-SSI and SSI models. The concept of Collapse Margin Ratio (*CMR*) was employed here to compare the performance of these models. It was shown that the SSI models typically collapsed at lower S_a levels. As a result, the collapse margin ratio values for the SSI models were smaller than their non-SSI counterparts.

This has led to a shift in fragility curves of SSI models to the left side of the non-SSI curves. It was shown in this study that for the soil condition considered here, neglecting the soil-structure interaction leads to under prediction of the probability of collapse and thus, results in a non-conservative design.

The approach presented in this study offers an insight into the response of structure-soil system subjected to severe failure loading. Such an approach can be employed in practice to adjust the non-SSI fragility curves to reflect the SSI effects.

6. Acknowledgements

The authors would like to thank Natural Sciences and Engineering Research Council of Canada (NSERC) for the support for this study. The authors are indebted to Mr. Don Kennedy, P. Eng., and Mr. Alfred Kao, P.Eng. of Associated Engineering for providing helpful bridge documents and drawings.

7. Copyrights

8. References

[1] Mitchell D, Brunea M, Williams M, Anderson D, Saatcioglu M, and Sexmith R. "Performance of bridges in the 1994 Northridge earthquake." Can. J. Civ. Eng. 22 (1995).

[2] Mylonakis G, Nikolaou A, And Gazetas G. "Soil-Pile-Bridge Seismic Interaction: Kinematic and Inertial Effects. Part I: Soft Soil." Earthquake Engineering and Structural Dynamics (1997): VOL. 26, 337-359.

[3] Mylonakis G, Gazetas G. "Seismic Soil-Structure Interaction: Beneficial or Detrimental?" Journal of Earthquake Engineering Vol. 4, No. 3 (2000): 277-301.

[4] Barbosa A, Mason B, And Romney K. SSI-Bridge: Soil-Bridge Interaction during Long-Duration Earthquake Motions. Final Project Report. Corvallis: Pacific Northwest Transportation Consortium (PacTrans), 2014.

[5] National Building Code of Canada (NBCC), (2015).

[6] FEMA P-695 (2009). In U. D. Security, Quantification of Building Seismic Performance Factors (pp. 6-12). Washington, D.C.: FEDERAL EMERGENCY MANAGEMENT AGENCY.

[7] Ashkani Zadeh K. Seismic Analysis of the RC integral bridges using performance-based design approach including soil structure interaction. Vancouver: The University of British Columbia, 2013. https://circle.ubc.ca/handle/2429/45407.

[8] SEISMOSOFT. (2014). SeismoStruct User manual for Version 7. Pavia-Italy: Seismosoft Ltd.

[9] CALTRANS. (2013). Abutments- Longitudinal Abutment Response. In C. D. (Caltrans), Caltrans Seismic Design Criteria - VERSION 1.7 (pp. 7-51, 7-52). Sacramento, California: CALTRANS.

[10] Allotey N, EL Naggar H. (2008). Generalized dynamic Winkler model for nonlinear soil-structure interaction analysis. Can. Geotech, 560-573.

[11] API (2007), Recommended practice for planning, designing, and constructing fixed offshore platforms, American Petroleum Institute. Section 6.8 Soil Reaction for Laterally Loaded Piles.

[12] Isenhower W.M., Wang S.D. L-Pile User's Manual for LPile 2013.

[13] Baker J.W, Cornell A. (2005). Vector Valued Ground Motion Intensity Measures for Probabilistic Analysis. PhD Theses, Stanford University, Civil and Environmental Engineering, Stanford.

[14] Vamvatsikos D, Cornell A (2002). Direct estimation of the seismic demand and capacity of MDOF systems through Incremental Dynamic Analysis of an SDOF approximation. 12th European Conference on Earthquake Engineering. London: 12th European Conference on Earthquake Engineering.

[15] Baker J.W. (2015) Efficient Analytical Fragility Function Fitting Using Dynamic Structural Analysis. Earthquake Spectra: February 2015, Vol. 31, No. 1, pp. 579-599.

[16] Hall B (2009). Geotechnical Memorandum for Leoran Brook Bridge No B5930 PMH1 Segment F1. Vancouver: Kiewit FLATIRON.

[17] Baker J.W. (2013). Research- Software and Data-Tools for fragility function fitting. Retrieved June 10, 2013, from Baker Research Group: http://www.stanford.edu/~bakerjw/fragility.html

[18] Mylonakis G (2000). The Role of Soil on the Collapse of 18 Piers of the Hanshin Expressway in the Kobe Earthquake. 12WCEE, 7.